# Automatic shoreline extraction based on remotely sensed Landsat imagery segmentation

**Nuno Matos**

Date:

Keywords:

Landsat, Arctic, automatic shoreline detection, image processing.

## Abstract

The detection and quantification of the changes on coastlines is very important to better understand the processes involved in its modification and consequently better predict future behaviors and derived environmental impacts. The common manual procedures used for delineations are preventing detailed inter- and intra-annual quantifications along extended Arctic coastlines. To overcome this issue, a methodology to automatically detect and extract coastlines on satellite imagery is presented. The evaluation of this approach is performed in the Yukon coast in the Canadian Arctic with a dataset constituted by satellite images acquired between 1986 and 2017.

## 1. State of art

Coastal regions are exceptionally sensitive to extreme meteorological conditions. Storms, thermal variations, permafrost degradation and decrease of sea-ice are the key factors for the current Arctic coastal erosion (Lantuit, 2012).

Landuit et al 2012, indicate a high probability about the Arctic coasts being world's region where the meteorological changes will have the biggest consequences. In addition, Kattsov et al 2005, forecast a severe air and ocean temperature increase, for the Artic most scenarios. Two direct consequences of temperature increase are the shorter time period with ice near the coast, allowing storms to stress the coast environment more time, together with and the twang of permafrost thawing (Lantuit, 2012). Those consequences change drastically the nutrients and sediments flow stressing the ecosystems and its biodiversity (Benjamin, 2009). Also, the communities are directly affected with losses of terrain and infrastructures degradation (Lantuit, 2012).

Recently there is a better knowledge about the Arctic coast, although it remains a region

that needs more research. This research needs to be suitable to the plausible and possible climate changes impact (Lantuit, 2012).

The Canadian Arctic coast changes are being quantified between periods of several years or even decades. Those kinds of evaluations do not allow verifying the coastal behavior within those periods. Therefore, it is necessary to invest on a systematic investigation with a circum-Arctic scale in order to get larger amounts of data to understand the dynamic evolution of all its coasts between shorter periods of time (for example annually). Consequently, it will help building more robust models to better forecast the coastal evolution and elaborate suitable and efficient risk preventing strategies (Lantuit, 2012) (Benjamin, 2009).

## 2. Study Area

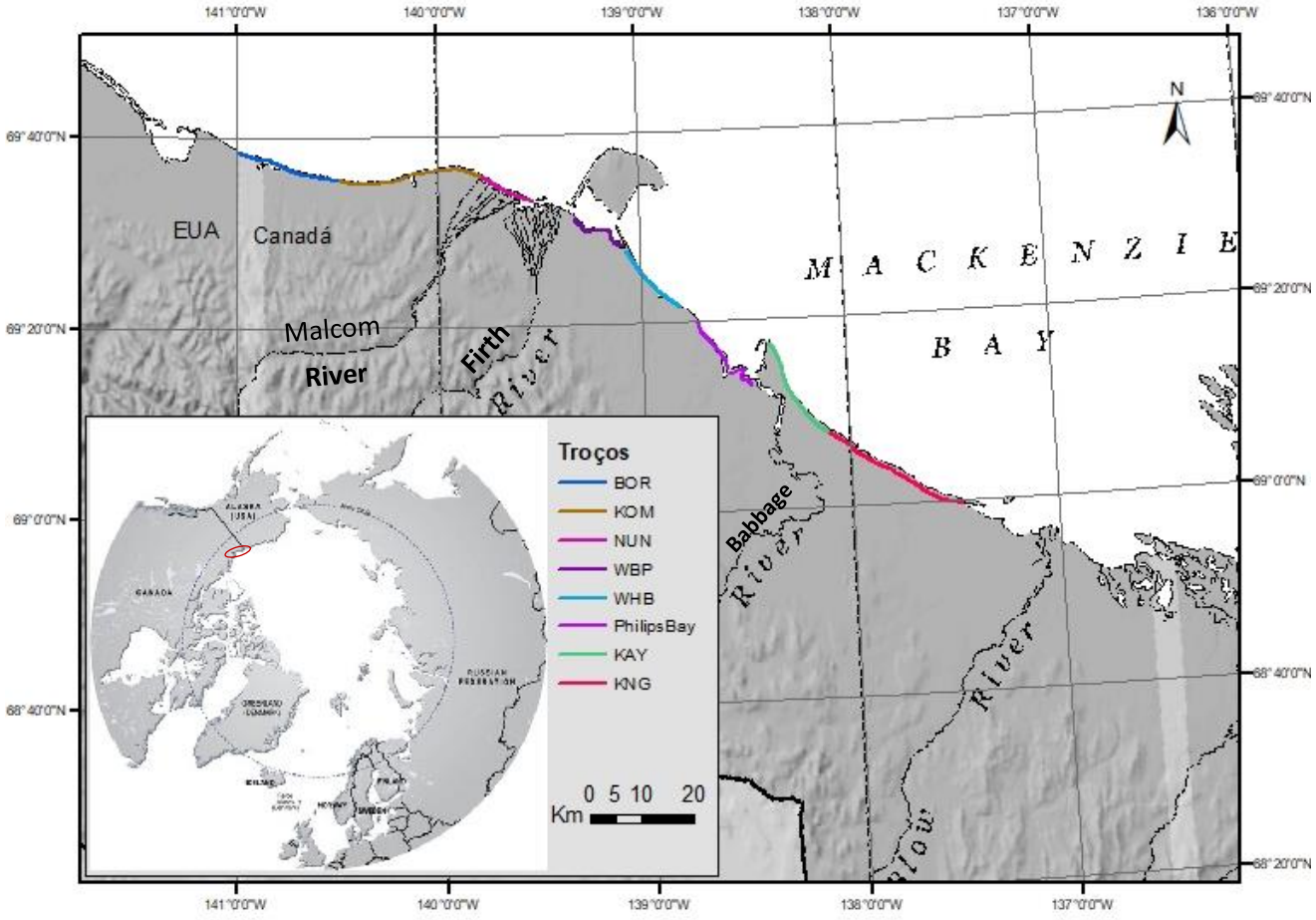


*fig 1 – Yukon coast limited by two light grey bars located between 141ºW and 137.5ºW a The 8 colored studied segments are: Border between Canada and USA (BOR), Komakuk beach (KOM), Nunaluk Spit (NUN), Workboat Passage (WBP), Whale Bay (WHB), Philips Bay, Kay Point (KAY) and king Point (KNG). The background map was obtained with 1:2500000 scale from the Yukon Environment State Department.*

The Yukon coast, fig 1, is characterized by a high content of continuous permafrost and ice, including ground-ice in a degradation state. Those characteristics give to the coast a big risk of erosion due to the temperature increasing leading to ice fusion. The region has an annual average temperature of -11 ºC and an annual average precipitation of around 200 and 300 mm (Couture, 2010). The studied coast starts on the west at BOR with cliffs with around 6 meters high, which turns shorter until Komakuk beach (KOM) where they reach about 3 meters. Along this extension of the coast it is possible to find up to 66% of ground ice (Couture, 2010). Next, Malcom and Firth bays are protected by a long chain of spits designated Nunaluk Spit (NUN) (Irrgang, 2018). The same characteristics can be found at Workboat Passage (WBP) near Herschel island. Between Whale Bay (WHB) and Babbage river stands a cliff with 3 meters which grow until a until 15 meters ice rich cliff at Whale Bay (WHB) (Irrgang, 2018). The segment of Kay Point (KAY) has cliffs up to 60 meters (Irrgang, 2018) that could have until 74% ground ice content (Couture, 2010)). Other authors, like Wolfe et al 2001 indicate the presence of different erosion phenomena like landslides and cracks on the ice due to thermal abrasion, in this last high cliff segment.

## 3. Data Collection

The pioneer online platform Google Earth Engine (GEE) was used to collect the freely available Landsat imagery (Table 1). In order to analyze the shoreline movement, images of 30 m/pixel captured by the satellites Landsat 5, 7 and 8, with the respective sensors TM, ETM+ e OLI, were used. Higher resolution images of 0.5 and 2 m/pixel from few sectors and one single year captured by Worldview2 satellite were also used.

There are two main reasons for using the Landsat datasets, the relatively large temporal distribution for the data collection and the free access to it. This study analyses data since 1986 until 2017. The satellite Worldview2 was chosen due to its higher spatial resolution and its availability through the H2020 European project Nunataryuk. The Worldview2 images are from two relatively small regions of the study area and although covering a short period of time, they have a big relevance for the methodology validation.

*Table 1-Collected pictures distributed for each studied coast segment*

| Troços | Imagens |
|---|---|
| BOR | 1993;1995;1998;2001;2002;2007;2010; 2013;2016;2017 |
| KOM | 1986;1990;1991;1993;1995;1998;2001; 2002;2003;2007;2009;2010;2013;2014; 2015; 2016;2017 |
| NUN | 1986;1990;1991;1993;1994;1995;1998; 2001;2002;2003;2004;2007;2009;2010; 2013; 2014;2015;2016;2017 |
| WBP | 1986;1990;1991;1993;1994;1995;1998; 2001;2002;2003;2004;2007;2009;2010; 2013; 2014;2015;2016;2017 |
| WHB | 1986;1990;1991;1993;1994;1995;1998; 2001;2002;2003;2004;2007;2008;2009; 2010; 2013;2014;2015;2016;2017 |
| Philips Bay | 1986;1988;1989;1990;1991;1993;1994; 1995;1998;2001;2002;2003;2004;2007; 2008;2009;2010;2013;2014;2015;2016; 2017 |
| KAY | 1986;1987;1988;1989;1990;1991;1993; 1994;1995;1998;2001;2002;2003;2004; 2007;2008;2009;2010;2013;2014;2015; 2016; 2017 |
| KNG | 1986;1987;1988;1989;1990;1991;1993; 1994;1995;1998;2001;2002;2003;2004; 2007;2008;2009;2010;2013;2014;2015; 2016; 2017 |

## 4. Methodology

After collecting the best images (atmospherically clear and with few or no ice-sea) covering the whole Yukon coast during summertime between 1986 and 2017 with GGE, they were processed using ENVI software, to automatically extract the shorelines of each image. ArcGIS was used for organizing all input datasets and for calculating and mapping the results obtained with the detection of the shorelines. The methodology workflow is represented in fig 2.

The shoreline was captured using the tool *feature extraction* available in ENVI. The *feature extraction* is an implementation of a methodology similar to the one explained by Meyer et al 1992 and Soille et al 2004. It has shown good results when applied by Husslander et al. (2012) to a coast delineation problem.

It has four main steps, like shown on fig 3. The first step consists on the simplification of the image, eliminating irrelevant minimums using morphological operations (opening/closing). It is mediated by the user with the 'Scale' parameter.

The second step is the simplified image's gradient construction. Its choice was turned to Sobel operator, selected as the best one out of four gradients: morphological gradient, internal morphological gradient, external morphological gradient and Sobel operator itself.

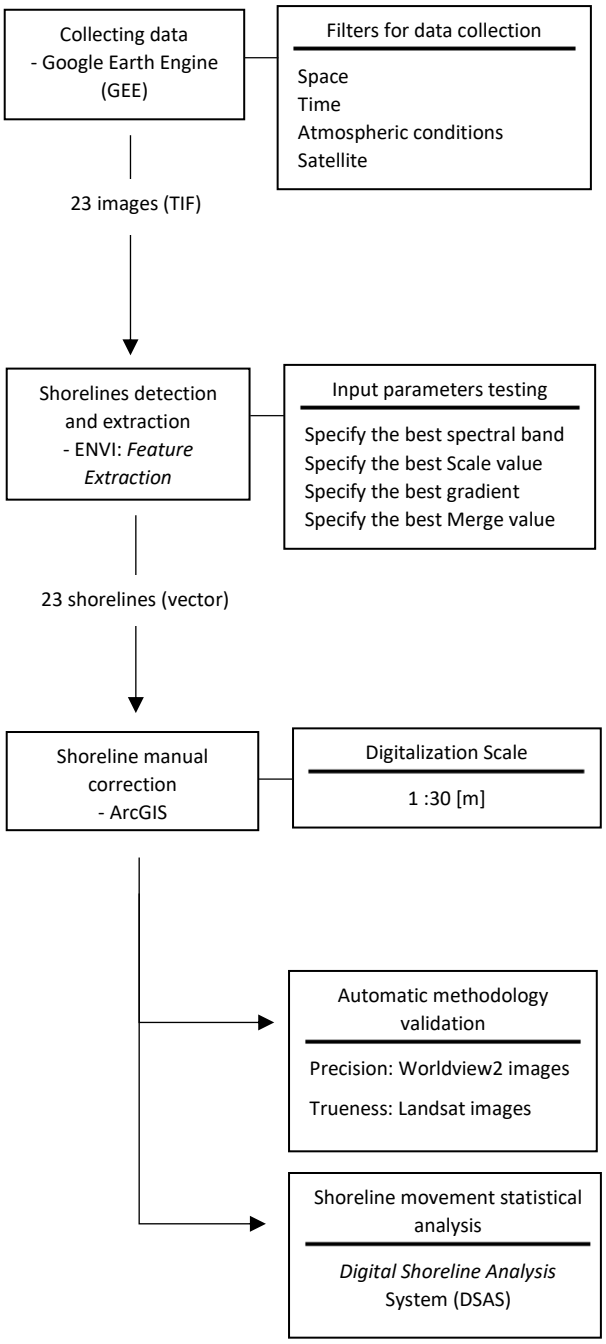


*fig 2 – Methodology workflow*

The third step is the gradient's segmentation with the morphological watershed transform. Following Meyer et al 1992, the application of the watershed transform in a gradient image instead of doing it directly to the image improves the detection of the transition regions present in the image. The segmentation result is an interconnected

line drawing, each one delineating the image different homogenous regions.(Roerdink, 2001), (Hamprecht, 2013) (Meyer, 1992).

The last step, a post-processing task, is intermediated by the user with the parameter 'Merge'. It merges the neighbor homogeneous regions (basins or objects) with similar characteristics.

The feature extraction results into a vector with a line that represents the shoreline. After obtaining the shoreline vectors they are manually corrected when necessary and overlayered. It is now possible to create a discrete representation of the shoreline movement between pairs of shorelines quantify a given the time period. To extract indicators and measurements from the shorelines, it was used a tool developed by the United States Geological Survey (USGS) which is Digital Shoreline Analysis System (DSAS). From that analysis 4 relevant indicators are obtained: Shoreline Change Envelope (SCE), Net Shoreline Movement (NSM), Net Point Rate (EPR) and Interannual Movement Analysis (IMA).

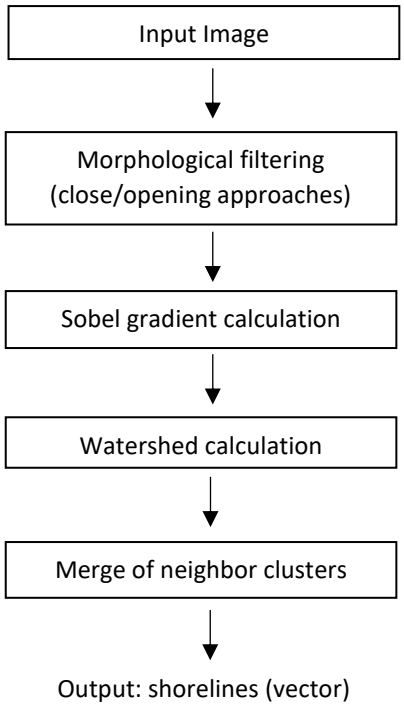


*fig 3 - Feature extraction workflow showing its 4 main steps*

## 5. Selecting parameters

The parameters tested as input in the methodology were the spectral band, the Scale value, the gradient and the Merge value. They were compared among each other in order to find which one leads to better results fitting the shoreline. The parameters were tested on one image from Landsat5 from 2010, in 3 different places of the coast, changing only one parameter at the time, keeping the others constant. After intensive testing the spectral band SWIR1, the value 63 for scale the gradient Sobel and the value 93 for Merge were selected.

Additional testing was performed to prove the selection's replication in images captured with a short period of time in between. Although the images were from the same

summer, they were captured in different periods of the day, with different illumination conditions and consequently producing different shadows. This evaluation allowed the calculation of the biggest deviation caused by the algorithm. This precision test was done in 2 long extensions of the coast obtaining the maximum value of 2m of error, which can be considered an excellent value. A trueness test was also performed with the WorldView2 high resolution images. To understand if the algorithm's results on Landsat images were fitting the shoreline, they were compared with other shoreline obtained through the high-resolution images in 4 smaller different regions. The quantification for the trueness error is 1.7m, the maximum value obtained in the 4 regions. Thus, considering the previous values and that the resolution of Landsat images is 30m, the accuracy of this method is 33.7m.

## 6. Results

After delineating the shorelines with the automated method for the Yukon coast along the 3 decades of analysis (1986-2017) it was possible obtain a series of results calculated with DSAS. This tool creates perpendicular transepts to the coast which intersect with distance the shorelines from each year. The transepts were set 90 meters from each other, representing a total of 1790 transepts. This metadata allows a multitemporal analysis.

Some abnormal areas were not considered for the analysis, due to the high concentration of sediments and the high rate of dynamic behavior (accretion and erosion) that area which is characteristic of spits and barrier islands. These low-level sediments do not allow to obtain images with high contrast (low values for the gradient) leading to shorelines with substantial digitalization errors. It is possible to see in fig 1 the segments where the analysis was made. NUN, Philips bay and STO are the 3 places analyzed only partially. Overall it was analyzed 161 km out of 210 km of shoreline (~76%).

The analysis outcome relies on 4 indicators the Shoreline Change Envelope (SCE), Net Shoreline Movement (NSM), End Point Rate (EPR) and Interannual Movement Analysis (IMA). The SCE computes the value of maximum distance between lines regardless their dates. it gives expression to places where the biggest movements, erosion or accretion had place. The NSM compares the oldest shoreline with the youngest (fig 4). The EPR divides the NSM per all years between the two lines. In Table 2 it is possible so see the last 3 indicators plus the *EPR which is the EPR calculated by Irrgang et al 2008 between 1950 and 2011 The IMA indicator gives the shoreline movement for the shortest periods of time possible in the data base (Table 3).

*Table 2 – Table with the segment's length (leng), % coastal coverage , indicators average per segment (SCE, NSM and EPR) and the average EPR presented by Irrgang et al 2018 (*EPR) relative to the period 1950 a 2011*

| | Leng [km] | % coverage | Average SCE [m] | Average NSM [m] | Average EPR [m/a] | *EPR [m/a] +/- 0.2 |
|---|---|---|---|---|---|---|
| BOR | 20.43 | 12.7 | 53.1 | -45.8 | -1.9 | -1.4 |
| KOM | 28.60 | 17.8 | 43.9 | -17.5 | -0.6 | -1.3 |
| NUN | 11.42 | 7.1 | 36.0 | 0.3 | 0.0 | -0.9 |
| WBP | 12.98 | 8.1 | 42.2 | -12.6 | -0.4 | -0.3 |
| WHB | 15.45 | 9.6 | 46.1 | -24.3 | -0.8 | -0.5 |
| Phillips | 19.64 | 12.2 | 73.0 | -13.8 | -0.4 | - |
| KAY | 21.79 | 13.6 | 61.3 | -19.8 | -0.6 | -0.2 |
| KNG | 30.20 | 18.8 | 52.4 | -20.4 | -0.7 | -0.5 |

The table above (Table 2) shows the segment BOR as the one with more erosion in the time period analyzed, with a significant difference when compared with the other segments. The SCE indicates Philips as the region with higher shoreline movement among all years. It makes sense since that region is the Babbage river estuary and so more prone to dynamic behaviors.

Table 3 gives the same indication as NSM and EPR through the IMA. The segment BOR is the one with higher annual erosion. It is also relevant highlight the erosion tendency shown by IMA, although some irregular results are present. A plausible cause for those irregularities is the presence of more waves near coast. The lines obtain in 1995 and 2016 have a bigger wave breaking zone then then images from the adjacent years.

*Table 3 – Results from the Interannual Movement Analysis (IMA) since 1986 until 2017. One the right side the year's average and in the bottom the segment's average.*

| Segment / Ano | BOR | | KOM | | NUN | | WBP | | WHB | | Philips | | KAY | | KNG | | Average [m] |
|---|---|---|---|---|---|---|---|---|---|---|---|---|---|---|---|---|---|
| | IMA [m] | % coverage | IMA [m] | % coverage | IMA [m] | % coverage | IMA [m] | % coverage | IMA [m] | % coverage | IMA [m] | % coverage | IMA [m] | % coverage | IMA [m] | % coverage | |
| 1987/1986 | | | | | | | | | | | 3.9 | 89 | -4.7 | 100 | 1.5 | 100 | **1.4** |
| 1988/1986 | | | | | | | | | 1.5 | 16 | | | | | | | |
| 1988/1987 | | | | | | | | | | | 3.9 | 96 | 8.0 | 100 | 1.8 | 100 | **4.6** |
| 1989/1986 | | | | | | | | | -4.3 | 54 | | | | | | | |
| 1989/1988 | | | | | | | | | | | -11.5 | 100 | -2.3 | 100 | -0.5 | 100 | **-6.7** |
| 1990/1986 | | | -2.5 | 55 | 0.1 | 98 | 3.6 | 100 | -4.6 | 100 | | | | | | | |
| 1990/1989 | | | | | | | | | | | 0.6 | 100 | -5.6 | 100 | -3.6 | 100 | **-1.5** |
| 1991/1990 | | | 7.6 | 47 | 1.3 | 98 | 0.5 | 100 | 1.8 | 100 | 1.8 | 100 | 2.3 | 100 | 4.2 | 99 | **2.5** |
| 1993/1991 | | | | | 6.4 | 99 | 3.5 | 100 | -1.2 | 100 | 1.8 | 100 | 0.8 | 100 | 5.1 | 98 | **2.9** |
| 1994/1993 | | | -14.8 | 70 | -8.2 | 99 | -8.6 | 100 | 2.2 | 100 | 3.0 | 100 | 3.1 | 100 | -3.9 | 100 | **-4.8** |
| 1995/1993 | 6.8 | 100 | 26.9 | 100 | | | | | | | | | | | | | |
| 1995/1994 | | | | | 5.7 | 99 | -1.2 | 100 | -28.4 | 100 | 22.1 | 100 | -36.1 | 100 | -10.7 | 98 | **-8.3** |
| 1998/1995 | -14.3 | 94 | -30.8 | 100 | -10.1 | 99 | 2.7 | 100 | 23.8 | 100 | 20.0 | 100 | 30.2 | 100 | 5.0 | 99 | **4.5** |
| 2001/1998 | -3.1 | 100 | 8.9 | 100 | 12.4 | 100 | 0.6 | 100 | -1.6 | 100 | 1.9 | 100 | -3.3 | 100 | 6.7 | 98 | **2.7** |
| 2002/2001 | 2.7 | 100 | -8.1 | 100 | -6.2 | 100 | -6.4 | 100 | -1.4 | 100 | 4.7 | 100 | 0.1 | 100 | 5.7 | 98 | **-2.4** |
| 2003/2002 | | | -4.4 | 40 | -5.4 | 100 | -5.5 | 100 | -1.7 | 100 | 2.1 | 100 | 6.8 | 100 | -2.2 | 99 | **-1.3** |
| 2004/2003 | | | -1.3 | 29 | -0.4 | 100 | 2.1 | 100 | -8.3 | 100 | -3.3 | 100 | -6.8 | 100 | -8.5 | 100 | **-3.7** |
| 2007/2002 | -11.4 | 100 | 4.4 | 100 | | | | | 6.1 | 100 | 1.2 | 100 | -2.5 | 100 | 6.3 | 98 | |
| 2007/2004 | | | | | 8.1 | 100 | 6.4 | 100 | | | | | | | | | **2.3** |
| 2008/2007 | | | | | | | | | -3.7 | 74 | 1.6 | 100 | 2.6 | 100 | -0.7 | 100 | **-0.1** |
| 2009/2007 | | | -20.9 | 45 | -7.9 | 100 | | | | | | | | | | | |
| 2009/2008 | | | | | | | -17.5 | 100 | -0.8 | 100 | 1.1 | 100 | -3.3 | 100 | -0.4 | 99 | **-6.7** |
| 2010/2007 | -7.8 | 100 | 4.0 | 100 | | | | | | | | | | | | | |
| 2010/2009 | | | | | 7.7 | 100 | 21.4 | 100 | 2.4 | 100 | 0.9 | 100 | -2.2 | 100 | 1.9 | 98 | **3.4** |
| 2013/2010 | -2.1 | 100 | -9.5 | 100 | -8.4 | 100 | -10.5 | 100 | -0.7 | 100 | 1.7 | 100 | 7.0 | 100 | 4.4 | 98 | **-2.0** |
| 2014/2013 | | | -3.7 | 42 | -2.4 | 100 | -8.3 | 100 | -2.9 | 100 | 5.5 | 100 | -7.3 | 100 | -8.6 | 100 | **-5.6** |
| 2016/2013 | 14.0 | 100 | 11.3 | 100 | | | | | | | | | | | | | |
| 2016/2015 | | | | | 18.9 | 100 | 10.2 | 100 | 16.9 | 100 | 3.7 | 100 | 8.5 | 100 | 4.6 | 98 | **10.0** |
| 2017/2016 | -31.4 | 100 | -13.6 | 100 | -12.5 | 100 | -6.2 | 100 | -22.0 | 100 | 9.1 | 100 | -17.4 | 100 | -2.3 | 98 | **-13.3** |
| **Average [m]** | **-5.2** | | **-2.9** | | **0.0** | | **-0.8** | | **-1.4** | | **-0.8** | | **-1.1** | | **0.3** | | **-1.1** / **-1.4** |

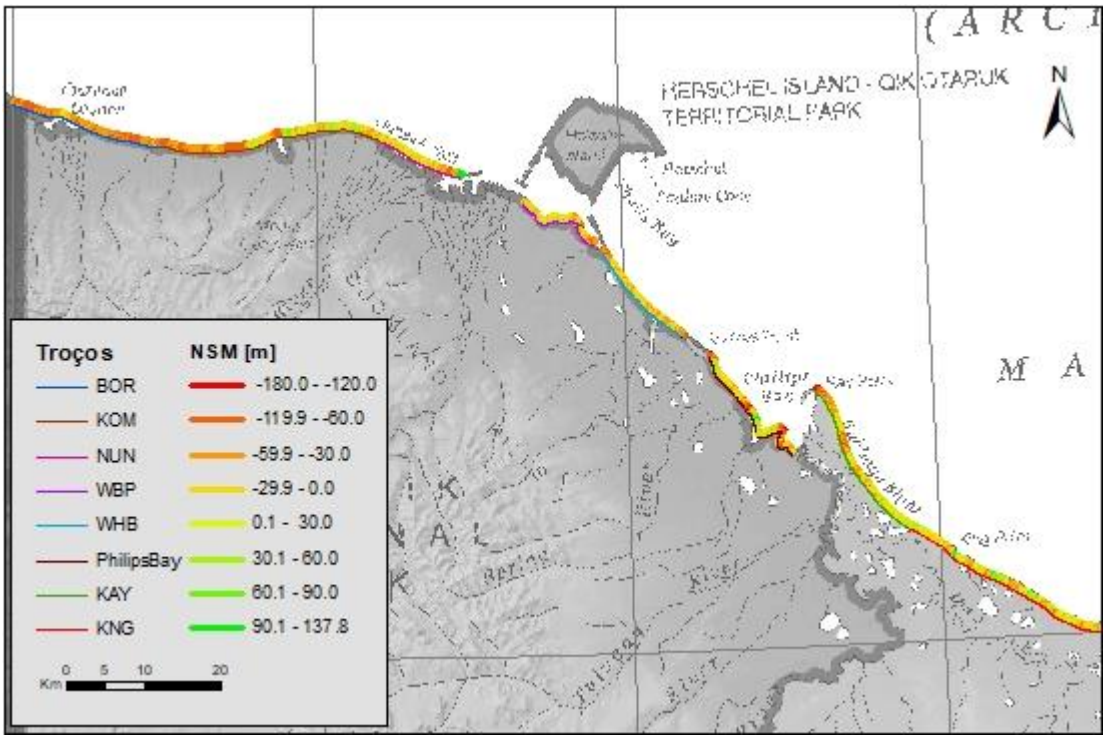


*fig 4 Yukon sea map with the illustration of NSM indicator*

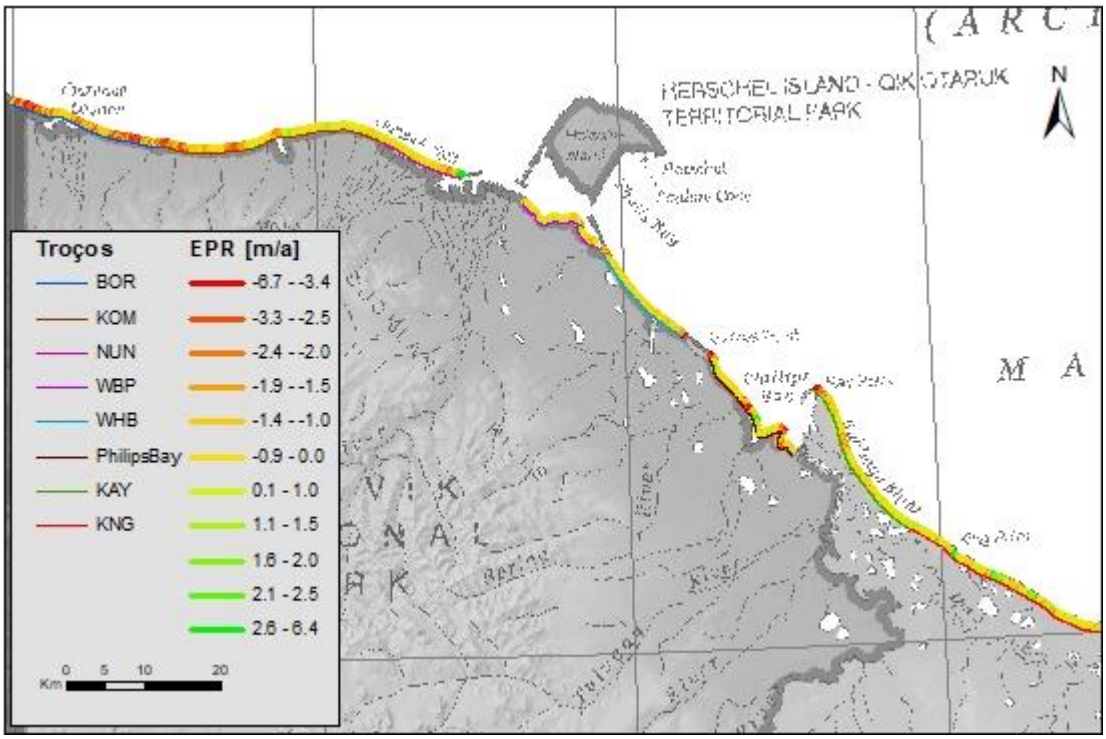


*fig 5 - Yukon sea map with the illustration of EPR indicator*

## 7. Conclusion

The Landsat images are suitable for shoreline detection and extraction with an accuracy of 33.7m. The proposed method reaches results similar with the ones shown by Irrgang et al 2018 only based on manual delineations and with few years analyzed. In this work, the shoreline movement results for the time period between 1986 and 2017 compare all extracted delineations. Some of them are not compared directly, the impossibility to know the relative position between shorelines imply the necessity to have one per year.

Although the utilization of this method for the whole Artic coast is a possibility, in this project the statistical analysis was only performed for 76% of the coast. This is due to the regions of spits and barrier islands which are not cooped in this analysis, since they refer to relatively rapid translation movements and not to the defined erosion or accretion. It should be advantageous to explore different approaches to study them separately. Also, the regions with more sediments deposition like Babbage river estuary and STO must be explored with higher resolution imagery in order to find more contrast level (higher gradient values). Those regions should be worked separately, as to calculate the accuracy associated to it and to categorize similar regions as to facilitate future analysis.

The results' analysis shows an erosive tendency with an average total rate of -0.72m/a approximately. The results also show a variation, depending on the segment analyzed where the segment BOR next to the border between USA and Canada is the one with bigger erosion rate, 2 m/a.

This method due to its automatic approach, allows an analysis in the shortest period available. The indicator IMA, the result of that application, fills a gap in the literature giving annually results which could possibly be helpful to understand better the behavior of the coast.

The possibility for replication of this method to all Artic coast is plausible and should be tried always with attention to the scale of the accuracy related with Landsat images.

## 8. References

Benjamin, M. J. (2009). Erosional history of Cape Halkett and contemporary monitoring of bluff . *Polar Geography vol 32*, pp. 129 - 142.

Couture, N. J. (2010). *FLUXES OF SOIL ORGANIC CARBON FROM ERODING PERMAFROST COASTS, CANADIAN BEAUFORT SEA.* Department of Geography, McGill University, Montreal.

Hamprecht, F. (2013). The image Analysis Class.

Hulslander, D. (2012). *Automated Mapping of Rapid Arctic Ocean Coastal Change Over Large Spans of Time and Geography*.

Irrgang, A. M. (26 de Abril de 2018). Journal of Geophysical Research: Earth Surface. *Variability in Rates of Coastal Change Along Yukon Coast, 1951 to 2015*.

Kattsov, V. M. (2005). *Future Climate Change: Modeling and Scenarios for the Arctic, chapter 4.* ACIA.

Lantuit, H. (Março de 2012). Estuaries and Coasts. *The Arctic Coastal Dynamics Database: A New Classification*.

Meyer, S. B. (1992). *The morphological Approach to Segmentation: The Watershed Trasformation*.

Roerdink, J. B. (2001). Fundamenta Informaticae. *"The watershed transform: definitions, algorithms, and parallelization strategies* .

S.A. Wolfe, E. K. (2001). Geological Survey of Canada Open File 4115. *Surficial characteristics and the distribution of thaw landforms (1970 to 1999), Shingle Point to Kay Point, Yukon Territory*.